



ELSEVIER

Available online at www.sciencedirect.com

Comparative Biochemistry and Physiology, Part C xx (2007) xxx – xxx

www.elsevier.com/locate/cbpc

Molecular and developmental effects of exposure to pyrene in the early life-stages of *Cyprinodon variegatus*

Laura A. Hendon, Erik A. Carlson, Steve Manning, Marius Brouwer*

Department of Coastal Sciences, Gulf Coast Research Laboratory, University of Southern Mississippi, 703 East Beach Drive, Ocean Springs, MS, USA

Received 21 July 2007; received in revised form 18 September 2007; accepted 18 September 2007

Abstract

Polycyclic aromatic hydrocarbons (PAHs) have been connected to developmental toxicity in the early life-stages of many species by their ability to bind to the aryl hydrocarbon receptor (AHR), which dimerizes with ARNT (AHR nuclear translocator) to induce transcription of genes such as *CYP1A1*. ARNT also dimerizes with HIF (hypoxia-inducible factor α) to induce transcription of genes such as *VEGF* (vascular endothelial growth factor), suggesting that PAHs may interfere with transcription of *VEGF* by competing for ARNT. Herein, we address the molecular and developmental effects of exposures to the weak AHR agonist pyrene on the early life-stages of the sheepshead minnow *Cyprinodon variegatus*. Embryos were exposed under flow-through conditions to 0, 20, 60, or 150 ppb pyrene up to 432 hours post-fertilization (hpf). RNA was extracted at 5 time points (12, 24, 48, 96, and 432 hpf) and changes in *CYP1A1* and *VEGF* expression were assessed by real-time RT-PCR. Since few genes have been documented for the sheepshead minnow, we first cloned and sequenced *CYP1A1*, *VEGF* and internal standard 18S *rRNA*. Pyrene significantly induced the AHR-regulated gene, *CYP1A1*, in a time- and dose-dependent manner, while pyrene failed to alter the HIF-regulated gene, *VEGF*. However, *VEGF* was found to change during various stages of normal development in this study. Although a normal hatch time (5 dpf) was observed for all treatments, pyrene-treated embryos showed dose-dependent abnormalities such as severe dorsal body curvature, mild pericardial and yolk-sac edema, and increased mortality. Taken together, these data indicate that embryonic exposure of sheepshead minnows to pyrene disrupts normal development and alters expression of an AHR/ARNT-regulated gene. In addition, embryonic exposure to pyrene failed to provide evidence of possible AHR-HIF pathway cross-talk since developmental expression of *VEGF* was unaltered. © 2007 Elsevier Inc. All rights reserved.

Keywords: Aryl hydrocarbon receptor; *Cyprinodon variegatus*; CYP1A; Developmental toxicity; Fish; Gene expression; Pyrene; VEGF

1. Introduction

Polycyclic aromatic hydrocarbons (PAH) are ubiquitous environmental contaminants that are primarily generated through anthropogenic activities such as incomplete burning of fossil fuels, oil, wood, and organic matter. They primarily enter the water column through land-based runoff (National Research Council, 2003) and get trapped within the sediments due to their hydrophobic nature. Disturbance of sediments will cause the release of the contaminants directly into the water column; therefore, marine animals that spend portions of their lives on or near the bottom may be directly subjected to the PAH

contamination. Since the early life-stages of many fishes take place in estuarine ecosystems, where PAH compounds are likely to be found, the occurrence of these environmental stressors in coastal waters may cause developmental and physiological toxicity to the early-life-stages of many marine species.

Organic contaminants that are primarily composed of PAHs have been connected to developmental toxicity in the early life-stages of many mammalian species by their ability to bind to the aryl hydrocarbon receptor (AHR) (reviewed by Hahn, 2002). The AHR is a ligand-activated transcription factor characterized by a basic helix-loop-helix motif and PAS (Per/ARNT/Sim) domain (Safe et al., 2000). Upon ligand binding, the AHR will translocate to the nucleus where it will heterodimerize with the AHR nuclear translocator (ARNT). This heterodimer complex can then bind to xenobiotic response elements (XREs) or dioxin response elements (DREs) located in the promoter region of various target

* Corresponding author. 703 East Beach Drive, Ocean Springs, MS 39564, USA. Tel.: +1 228 872 4294; fax: +1 228 872 4204.

E-mail address: marius.brouwer@usm.edu (M. Brouwer).

genes, such as *CYP1A1*, *CYP1A2*, or *CYP1B1* (Denison et al., 2002; Nebert et al., 2000; Schmidt and Bradfield, 1996), resulting in alterations in gene expression.

AHR's partner protein ARNT can also recognize the transcription factor hypoxia-inducible factor 1- α (HIF 1- α) (Semenza, 1999). Once activated, the HIF 1- α /ARNT dimer complex can bind to hypoxia response elements (HREs) in target genes, such as erythropoietin (*EPO*) (Semenza and Wang, 1992), vascular endothelial growth factor (*VEGF*) (Forsythe et al., 1996; Semenza, 2000) and heme oxygenase (Lee et al., 1997; Morita et al., 1995). *VEGF* has been characterized in various teleost fish such as *Danio rerio* (zebrafish) and *Fugu rubripes* (pufferfish) (Gong et al., 2004), in *Xenopus laevis* (African clawed frog), *Gallus gallus* (chicken), and mammals (Holmes and Zachary, 2005). It takes on the crucial role of vascularization in embryonic development and can induce angiogenesis by controlling the growth and formation of blood vessels both in normal development and in ischemic or inflamed tissues, such as during tumor growth or tissue repair (Holmes and Zachary, 2005). Recently, Ivnitski-Steele and Walker (2003) showed a reduction in *VEGF* mRNA and protein expression in TCDD-treated chicken embryo hearts. In contrast, Prasch et al. (2004) demonstrated a significant increase in transcription of the HIF-regulated gene, heme oxygenase, in TCDD-treated embryonic zebrafish. Since hypoxia-induced genes appear to be altered by AHR ligands, and since ligand-activated AHR may sequester ARNT from HIF-mediated pathways, we wanted to determine if a weaker AHR agonist could alter *VEGF* expression in embryonic fish.

While stronger AHR agonists such as benzo[a]pyrene (BaP) or 2,3,7,8-tetrachlorodibenzo-p-dioxin (TCDD) are generally used as compounds for toxicity studies, we chose to use the common PAH pyrene, because it has been found at high concentrations in coastal estuarine sites that have been affected by creosote and other hazardous environmental pollutants which may directly influence marine and estuarine animals (US EPA, 2000, 2006). In fish species, pyrene is considered to be a far weaker AHR agonist than other more potent PAHs such as BaP (Barron et al., 2004). In spite of this, pyrene-induced developmental toxicity should reflect its ability to activate the AHR pathway given that toxic responses to PAHs in other species have been a direct result of the compound's ability to activate AHR (Nebert et al., 2000). Supporting this notion, Incardona et al. (2004) demonstrated that zebrafish embryos exposed to pyrene exhibit toxicity endpoints similar to stronger PAHs, such as pericardial edema, failed swim bladder inflation, anemia, and mortality. Further resembling the effects of other AHR agonists, *CYP1A* levels were elevated in adult mummichogs (*Fundulus heteroclitus*) when exposed to pyrene (Roling et al., 2004).

In embryonic fish, little is known about the individual effects of PAH compounds and the mechanisms that underlie their mode of action. Zebrafish are generally used as the model organism since a functional AHR pathway has already been identified for this species (Andreasen et al., 2002a). For this current study, we chose to use *Cyprinodon variegatus*, a small teleost fish indigenous to the Atlantic and Gulf coasts of the United States. Due to its chemical sensitivity and its ability to be easily bred and

reared in laboratory conditions, the Environmental Protection Agency (EPA) has adopted the sheepshead minnow as the standard laboratory test organism for studying pollution levels in effluents discharged into marine and estuarine waters (US EPA, 2002). However, despite its importance as an estuarine small fish model for toxicity testing, little information exists regarding the developmental/molecular responses during PAH exposure. More specifically, there have been few if any reports pertaining to the effects of the AHR agonist pyrene on the embryonic or larval stages of any estuarine-resident species. Since eggs laid by these daily spawners are often dispersed in substrata on or near the estuarine floor (Kuntz, 1916), PAH exposure may pose a potential risk to *C. variegatus* embryonic development. To address these issues, this current study utilized real-time RT-PCR to assess genes altered in the pyrene response of the embryonic sheepshead minnow. In addition, we examined the developmental toxic effects of exposures to pyrene both in the embryonic and larval stages to illustrate the potential consequences of long-term pyrene exposure (432 hpf) on the early-life-stages of *C. variegatus*.

2. Materials and methods

2.1. Test animals

Sheepshead minnows (*C. variegatus*) are small (35–50 mm) oviparous euryhaline fish that are indigenous to the Atlantic and Gulf of Mexico coasts of the United States. Lab-reared *C. variegatus* used for cloning and sequencing were from original broodstock obtained from the Environmental Protection Agency in Gulf Breeze, FL. Wild-caught adult sheepshead minnows used in the pyrene exposure were collected from estuarine waters in Davis Bayou (30°23'04.51"N; 88°46'05.57"W; Ocean Springs, MS). Fish used in this study were ~1–2 years old. All fish were maintained at 27 °C in 15 g/L salinity artificial seawater (Fritz, Mesquite, TX) for at least 7 d prior to test initiation. Embryos were obtained via means of artificial fertilization according to the procedures described by the US EPA (2002). Fertilized eggs were collected within 1 to 1.5 h post-fertilization (hpf), pooled, and placed into clean, artificial seawater. Embryos used in this study were kept under 16 h:8 h light:dark conditions for 432 hpf and tank pH, temperature, salinity, and DO (~8 mg O₂/L) were monitored daily for all treatments.

2.2. Fish sacrifice and total RNA isolation for cloning

All fish were euthanized by a brief cold shock (~1–5 min) followed by rapid decapitation. Fish used in *CYP1A1* cloning were exposed to 200 ppb pyrene for 24 h under flow-through conditions (Manning et al., 1999) prior to tissue extraction. All excised liver and heart tissue samples were placed in 1 mL of RNAlater (Ambion, Austin, TX, USA) and stored at 4 °C. For isolation of total RNA, liver and heart tissue samples were homogenized in 750 μ L of RNA-STAT 60 reagent (Tel-Test, Friendswood, TX, USA). Following homogenization, RNA was extracted by 2 rounds of reagent treatment according to the manufacturer's instructions. Following the second extraction, RNA was precipitated overnight in 100% isopropanol, pelleted

at 12,000 ×g at 4 °C for 1 h, and washed twice in 75% ethanol. The washed RNA pellets were then resuspended in 50 μL RNA storage solution (Ambion) and subjected to TURBO DNase I (Ambion) treatment to avoid amplification of contaminant genomic DNA. Following DNase treatment, all total RNA was precipitated overnight in 3 M NaOAc and 100% ethanol, pelleted at 12,000 ×g at 4 °C for 30 min, and washed with 75% ethanol. The washed pellets were then resuspended in 50 μL RNA storage solution (Ambion). The purity and quantity of the resulting RNA were determined using the NanoDrop ND-1000 spectrophotometer (NanoDrop Technologies, Wilmington, DE, USA). All total RNA samples used in this study possessed a 260/280 nm ratio greater than 1.8. To further confirm the purity and integrity of the total RNA, each sample was analyzed using the 2100 Bioanalyzer and RNA 6000 Nano Chip kit (Agilent Technologies, Palo Alto, CA, USA). All samples used in this study possessed distinct bands with a 28S/18S ratio greater than 1.0. All total RNA samples were stored at –80 °C until use.

2.3. Reverse transcription and PCR amplification for cloning

First-strand cDNA was produced from 2 μg of total RNA for each sample using Superscript 1st-Strand cDNA Synthesis Kit (Invitrogen, Carlsbad, CA, USA) with random hexamer primers in 20 μL volumes according to the manufacturer's instructions. RNase H (1 μL) (Invitrogen) was used to remove any last traces of RNA. First-strand cDNA was amplified using degenerate (CYP1A, VEGF, AhR) primers (Table 1) designed from conserved nucleotide sequences identified using Clustal W version 1.7 multiple sequence alignment program, or from amino acid sequences using the Block Maker (Henikoff et al., 1995) and Consensus-Degenerate Hybrid Oligonucleotide Primers program (CODEHOP; Rose et al., 1998). QuantumRNA Universal 18S Internal Standards were used as primers for 18S rRNA (Ambion). Briefly, 2 μL of the reverse transcribed product was added to 17.75 μL sterilized water, 2.5 μL 10×PCR Buffer, 0.5 μL 10 mM dNTP mix, 0.25 μL Taq polymerase and 1 μL 10 μM each of forward and reverse primer (Table 1). PCR for each gene's primers were set up as follows: pre-denature at 94 °C for 1 min, (denature: 94 °C for 30 sec, anneal: melting temperature of desired primers for 30 s, extend: 72 °C for 1 min) × 35 cycles, then 5 min at 72 °C, and hold at 4 °C. Two successive PCRs were used for each gene of interest except 18S rRNA. One PCR for the isolation of 18S rRNA

was utilized with an annealing temperature of 60 °C. For *AHR*, *CYP1A*, and *VEGF*'s first PCR, a gradient of twelve annealing temperatures was used with their corresponding forward and reverse primers (Table 1). A gradient of 43 to 60 °C was applied to the *AHR* primers, while gradients of 55 to 65 °C and 49 to 59 °C were chosen for *VEGF* and *CYP1A* genes, respectively. Each gene's second PCR, forward and nested reverse primers (Table 1) were used and applied to 2 μL of the PCR product from the first PCR. An annealing temperature of 55 °C was chosen for *AHR* and *VEGF*'s second PCR, while a temperature of 49 °C was used with *CYP1A* primers. Five-microliter aliquots of each reaction were then analyzed on 1.5% agarose gels.

2.4. Cloning and sequencing of PCR-amplified cDNA

PCR products (50 μL reactions) were separated by size through electrophoresis on 2% agarose gels. Desired bands were excised under UV light and gel purified using QIAquick Gel Extraction Kit (QIAGEN). Purified products were ligated into the pGEM-T® Easy Plasmid/Vector System (Promega) with T4 DNA ligase. JM109 High Efficiency Competent Cells (Promega) were transformed with 2 μL of ligation mixture and plated on LB-Amp plates containing X-gal and IPTG. White (positive) colonies were selected for extraction/purification of vector DNA using Wizard® Plus Minipreps DNA Purification System (Promega). Purified vectors were screened for the appropriate insert by restriction digestion with *EcoRI* followed by agarose gel (1.5%) electrophoresis. Clones containing the appropriate insert were selected and sequenced using the CEQ 8000 DNA Sequencer (Beckman Coulter, Fullerton, CA, USA) according to the manufacturer's instructions. All sequences were Blast searched in order to confirm that each sequence corresponded to the gene of interest.

2.5. Waterborne exposure of embryos to pyrene

Pyrene (98% purity) was purchased from Acros Organics and dissolved in dimethylsulfoxide (DMSO) (>99% purity) to give a final concentration of 2 mg/L DMSO. 2500 sheepshead minnow embryos (~4 hpf) were exposed to seawater, vehicle (0.1% DMSO), or nominal concentrations of pyrene (20, 60, and 150 μg/L) in 5 gallon glass tanks using a semi-flow-through exposure system (4 × 500 mL additions/tank/h or 95% replacement/tank/d) similar to that described by Manning et al. (1999).

t1.1 Table 1

t1.2 Degenerate primers utilized in cloning and sequencing

t1.3 Gene name	Symbol	Primer	Sequence (5'→3')	<i>T_m</i> (°C)
t1.4 Aryl hydrocarbon receptor	AHR	Forward	AARTCSAAYCCNTCCAAACG	54.3
t1.5		Nested reverse	GTKCKKATCTCCARNATGGA	53.0
t1.6		Reverse	GCTGCATGGATGAACTGATA	52.6
t1.7 Cytochrome P450 1A	CYP1A	Forward	GTNGCNAAYGTNATHTYGG	53.8
t1.8		Nested reverse	CARTGNGGDATNGTRAANGG	53.0
t1.9		Reverse	CATNGTNARNCCRTAYTCNGG	54.1
t1.10 Vascular endothelial growth factor	VEGF	Forward	CGAGATGCTGGTGGACATCTTHCARGARTAYC	62.4
t1.11		Nested reverse	GCACCTTGCAAGTCTGGGRTCYTGNAC	65.7
t1.12		Reverse	CCGGCAGGTCCGCTCRTTARYTC	63.9

Embryos were randomly separated into 4 replicate tanks for each exposure group (seawater, vehicle, pyrene at 20, 60, and 150 $\mu\text{g/L}$) at a density of 125 embryos/tank, for a total of 20 aquaria for the 5 individual treatments. Embryos were retained in embryo cups constructed from 350 micron nylon mesh screen silicined to a Petri dish (13.5 \times 10 cm). Each cup contained 25 embryos. At 12, 24, 48, 96, and 432 hpf, twenty-five embryos from each tank were removed from the water and served as sources for total RNA. Embryos were observed every twenty-four hours and scored for the presence/absence of yolk-sac/pericardial edema, dorsal body curvature, and abnormal growth in the head and trunk region using a Leica MS5 dissecting microscope (Leica, Bannockburn, IL, USA) and Sony DSC F-717 CyberShot digital camera (Sony, New York, NY, USA). For observations, embryos were removed from the tanks, scored in their surrounding water, and returned to the test system within 5 min. Prior to termination, digital images were taken at 432 hpf (18 dpf) of all remaining fry using a Panasonic GP-KR 222 digital camera (Panasonic, Secaucus, NJ, USA) fitted with a TV Zoom Lens F2.5 (18–108 mm). Standard length measurements were then obtained from the digital images using Image Processing and Analysis in Java.

2.6. Total RNA isolation for pyrene exposure

All fry (432 hpf) were placed in 1 mL RNAlater (Ambion) and stored at 4 °C. RNA was extracted and analyzed as previously described. Final pellets were resuspended in 10 μL RNA storage solution (Ambion). All total RNA samples were stored at –80 °C until use.

2.7. Real-time RT-PCR

Relative levels of *CYP1A1* and *VEGF* in pyrene-treated embryos and fry were measured using Q-PCR. First-strand cDNA was produced as described above. Aliquots (2 μL) of the resulting RT reactions were then subjected to real-time RT-PCR using an iCycler thermal cycler (Biorad, Hercules, CA, USA), the appropriate gene-specific primers, and SyBr Green Supermix kit (Biorad) according to the manufacturer's instructions. Real-time RT-PCR reaction conditions were set up as follows: pre-denature at 94 °C for 1 min, (denature: 94 °C for 30 s, anneal: 56 °C for 30 s, extend: 72 °C for 1 min) \times 35 cycles, then 5 min at 72 °C, and hold at 4 °C. For normalization, real-time RT-PCR was conducted with primers for 18S Ribosomal RNA (18S rRNA) for each sample. Each target gene's Ct values came out within ~10 cycles of the 18S gene, demonstrating that each gene was more or less present in similar overall abundances. Samples were run in duplicate for each primer set with each

reaction having a total volume of 50 μL . Sense and antisense gene-specific primers were designed from the cloned sequences previously described using Beacon Designer 2.0 software (Premier Biosoft International) (Table 2). A standard curve for each gene was performed by pooling cDNA samples and analyzing a 1:5 dilution series. The relative starting quantity (SQ) of each sample was assessed against the standard curve for that gene and compared to the internal housekeeping gene 18S rRNA (Achenbach et al., 2004).

2.8. HPLC analysis of pyrene

Pyrene was measured in water samples taken from all aquaria prior to test initiation. For the exposure, pyrene was measured by taking water samples from two aquaria per treatment twice weekly (4 measurements/treatment/week). Pyrene was measured using a Beckman HPLC System Gold 126 equipped with a C-18 reverse phase column (4.6 mm \times 25 cm), which was developed using 90% acetonitrile at a flow rate of 0.8 mL/min for 16 min. Pyrene in the column effluent was detected with a Jasco FP-920 fluorescence detector (Easton, MD) using an excitation wavelength of 235 nm and an emission wavelength of 390 nm. Acetonitrile (HPLC grade) was purchased from Fisher Scientific and was reported by the supplier to be at least 99.9% pure. The solvent was diluted to 90% using filtered nanopure water prior to test runs.

The instrument was calibrated with an 8-point curve using standards (1, 5, 10, 25, 50, 100, 150, and 200 ppb) prepared from a 2000 ppm pyrene stock solution and filtered dilution water. The pyrene concentration was calculated with $x = (y - z) / m$, where x is the water sample, y is the area under the pyrene peak, z is the intercept, and m is the slope of the curve.

2.9. Statistics

All statistical analyses and graphing were done with SPSS 13.0, SigmaStat 3.1, and/or Microsoft Excel SP2 for Windows. Biological endpoints i.e. % hatch, % survival (pre- and post-hatch), % developmental abnormalities, and standard length measurements were arcsine square root transformed (arcsine (\sqrt{x})) before determining significant differences. Kruskal-Wallis (KW) ANOVA on Ranks was performed to evaluate differences in standard length measurements based on individual treatment groups, followed by Dunn's post-hoc test. Percent hatch and % survival (pre- and post-hatch) were analyzed via ANOVA or KW ANOVA on Ranks followed, by Tukey or Student–Newman–Keuls (SNK) post-hoc test. Q-PCR data normally distributed and with homogeneity of variance were assessed via ANOVA, followed by Tukey or Dunnett post-hoc tests. Q-PCR data with

t2.1 Table 2

t2.2 Gene specific primers utilized in quantitative real-time RT-PCR

t2.3 Gene name	Symbol	Product length (bp)	GenBank ID	Sense primer (5'→3')	Anti-sense primer (5'→3')
t2.4 18S ribosomal protein	18S rRNA	101	EF535030	GCTGAACGCCACTGTCC	ATTCGATAACGAACGAGACTC
t2.5 Cytochrome P450 1A	CYP1A1	139	EF535032	GCAGATTAACCACGACCCAGAG	GCATCGCCTCCTTCTAAGC
t2.6 Vascular endothelial	VEGF	105	EF535031	AGCACATCTTATCCCATCCTG	CCATTGTGACGTTACGAGTTTC

333 heterogeneity of variance and/or not normally distributed were
 334 assessed via KW ANOVA on Ranks, followed by SNK post-hoc
 335 test. Results are presented as mean±SEM. In all cases, a *p*-
 336 value ≤ 0.05 was regarded as significantly different from control.

337 3. Results and discussion

338 3.1. PCR amplification, cloning and sequencing of *AHR2*, 339 *VEGF*, *CYP1A1*, and *18S rRNA*

340 The primary goal of this research was to determine if pyrene
 341 could activate the AHR pathway, and induce *CYP1A* expression in
 342 embryonic sheepshead minnows, with concomitant increase of
 343 developmental toxicity. Since few genes have been described for
 344 the sheepshead minnow, we first cloned and sequenced fragments
 345 of sheepshead minnow *AHR2*, *CYP1A1*, *VEGF*, and *18S rRNA*
 346 genes using degenerate primers based on sequences of
 347 corresponding genes in other fish and mammalian species (Table 1).

348 The *AHR* gene was cloned and sequenced in order to
 349 ascertain that the *AHR2* isoform that serves as the PAH and
 350 TCDD receptor in other fish species (Andreasen et al., 2002a;
 351 Tanguay et al., 1999) was present in *C. variegatus*. The
 352 sequence of the other genes was used for the design of gene-
 353 specific primers for Q-PCR. PCR amplification products of 688,
 354 281, 516, and 322 bps were obtained for *AHR2*, *VEGF*,
 355 *CYP1A1*, and *18S rRNA* genes, respectively. NCBI Blastx
 356 search confirmed that each translated nucleotide sequence
 357 corresponded most closely to partial amino acid sequences of
 358 *AHR2*, *VEGF*, *CYP1A1* from other fish species. The *AHR2*
 359 sequence of *C. variegatus* (GenBank Accession no. EF535033)
 360 was most similar to the *AHR2* amino acid sequence of *F.*
 361 *heteroclitus* (mummichog; 93% identities). The *VEGF* se-
 362 quence of *C. variegatus* (GenBank Accession no. EF535031)
 363 most closely resembled the *VEGF* amino acid sequence of
 364 *Epinephelus coioides* (orange-spotted grouper; 77% identities).
 365 The sequence of *CYP1A1* (GenBank Accession no. EF535032)
 366 was most similar to *CYP1A1* amino acid sequences of *Kryp-*
 367 *tolebias marmoratus* (mangrove rivulus; 90% identities), and *F.*
 368 *heteroclitus* (mummichog; 90% identities). *18S rRNA* of *C.*
 369 *variegatus* (GenBank Accession no. EF535030) showed 96%
 370 identity with *18S* nucleotide sequence of several fishes.

371 3.2. Specificity and efficiency analysis of gene specific primers

372 Using the determined sequences, sense and antisense gene-
 373 specific primers were designed for *VEGF*, *CYP1A1*, and *18S*
 374 *rRNA* genes, respectively (Table 2).

375 To determine the specificity of each primer set, cDNA (2 μL)
 376 of *C. variegatus* was PCR amplified and electrophoresed on a
 377 1.5% agarose gel. *18S rRNA*, *VEGF*, and *CYP1A1* PCR
 378 products showed single bands with the size of each band
 379 corresponding to the predicted values. To verify the PCR
 380 efficiency of each primer set, real-time RT-PCR was performed
 381 using 5 fivefold cDNA dilutions. The correlation coefficient of
 382 each standard curve was ~0.998. The PCR efficiency,
 383 calculated from the slope of each standard curve, was 102.3%
 384 (*18S*), 101.4% (*VEGF*), and 93.4% (*CYP1A1*).

385 3.3. Pyrene concentrations

386 Embryonic sheepshead minnows, within 4 hpf, were
 387 exposed to seawater, vehicle, 20, 60, or 150 ppb pyrene for
 388 432 hpf. Analyzed water samples overall showed small
 389 oscillations in pyrene concentrations. The average measured
 390 concentrations of the three exposure treatments (16.3, 42.6, and
 391 117.4 ppb) were 19–29% lower than the targeted nominal
 392 concentrations of 20, 60, and 150 ppb; however, all three
 393 treatments increased in a statistically significant manner with
 394 dose (Table 3).

395 Reduced pyrene concentrations in the water may be due to
 396 photo-degradation of the pyrene stock solution, absorption by
 397 the embryos or larvae, or adsorption to the glass aquaria,
 398 delivery lines, or other parts of the test system.

399 3.4. Effect of pyrene exposure on PAH-inducible gene 400 expression

401 To examine if pyrene could activate the AHR pathway,
 402 expression of the PAH-inducible gene, *CYP1A1*, was measured
 403 in embryos treated with seawater, vehicle, or pyrene (20, 60,
 404 150 ppb) starting at ~4 hpf for 432 hpf. Since it is not known
 405 when during development the AHR/ARNT pathway in
 406 sheepshead minnows is established, expression levels were
 407 measured both in the embryonic (12, 24, 48, 96 hpf) and larval
 408 (432 hpf) stages.

409 Although pyrene is considered to be a far weaker AHR agonist
 410 than other potent AHR ligands in fish (Barron et al., 2004),
 411 pyrene-induced developmental toxicity should reflect its ability to
 412 activate the AHR pathway given that PAH-mediated toxic
 413 responses in other species have been a direct result of the
 414 compound's ability to activate the AHR (Nebert et al., 2000). In
 415 zebrafish, medaka, and lake trout, *CYP1A* is highly inducible
 416 following embryonic exposure to TCDD (Andreasen et al., 2002b;
 417 Guiney et al., 2000). Thus, we chose *CYP1A* to serve as a
 418 biomarker of AHR activation in pyrene-exposed sheepshead
 419 minnow embryos. In all instances, seawater and vehicle treatments
 420 showed no significant differences in *CYP1A1* expression;
 421 therefore, for all time points, expression of *CYP1A1* was solely
 422 based on differences between vehicle and pyrene treatments. Real-
 423 time RT-PCR showed that *CYP1A1* was a pyrene-inducible gene
 424 both in the embryonic and larval stages as early as 24 hpf (Table 4).

425 Interestingly however, *CYP1A1* was undetectable for all
 426 treatment groups regardless of pyrene dosage at 12 hpf. It was

Table 3
 Measured pyrene concentrations in the water after exposing embryonic
 sheepshead minnows for 432 hpf

Nominal pyrene concentration (ppb)	Measured pyrene concentration (ppb)	
Seawater	Not detected	t3.4
Vehicle	Not detected	t3.5
20	16.3±6.4	t3.6
60	42.6±7.9	t3.7
150	117.6±14.3	t3.8

Data are expressed as mean±standard deviation (*n*=20). Each measured pyrene
 concentration is statistically different from all other pyrene treatments as
 determined by ANOVA, followed by Tukey post-hoc test (*p* ≤ 0.05).

t4.1 Table 4

t4.2 *CYP1A1* normalized fold-change of pyrene-exposed *C. variegatus*

t4.3	Time	DMSO	20 ppb pyrene	60 ppb pyrene	150 ppb pyrene
t4.4	12	nd	nd	nd	nd
t4.5	24	1.00±0.4	2.92±1.9	6.18±1.1 ^a	5.23±2.5 ^a
t4.6	48	3.37±0.4 ^x	6.54±1.1 ^x	8.67±1.3 ^{a x}	19.30±4.5 ^{abc x}
t4.7	96	6.15±0.9 ^{xy}	18.30±5.6 ^{a xy}	35.90±7.7 ^{ab xy}	88.80±22 ^{abc xy}
t4.8	432	45.90±3.2 ^{xyz}	79.10±27 ^{a xyz}	182.00±36 ^{ab xyz}	m

CYP1A1 normalized fold-change measured using Q-PCR relative to 12 hpf DMSO treatment. Data is presented as mean starting quantity (SQ) [*CYP1A1*/18S] ($n=4$).

t4.9 m — 100% mortality before conclusion of exposure at 432 hpf.

t4.11 nd — not detected by Q-PCR.

Changes among treatments at same time points:

^a Significantly different from same day DMSO treatment.

^b Significantly different from same day 20 ppb pyrene treatment.

^c Significantly different from same day 60 ppb pyrene treatment.

t4.12

Changes within treatments over time:

^x Significantly different from same treatment at 24 hpf.

^y Significantly different from same treatment at 48 hpf.

t4.13 ^z Significantly different from same treatment at 96 hpf.

not until 24 hpf, that results showed a dose-dependent relationship with increasing *CYP1A1* expression among pyrene treatment groups. At 48 hpf, *CYP1A1* expression was up-regulated 1.9-, 2.6-, and 5.7-fold in the 20, 60, and 150 ppb treatments, respectively, relative to same day vehicle control. The pyrene-dependent induction continued to increase over time, so that at 96 hpf the 20, 60, and 150 ppb pyrene-treated groups showed *CYP1A1* levels that were induced 3-, 5.8-, and 14.4-fold over same day vehicle-treated controls. Prasch et al. (2004) showed a similar pattern in *CYP1A1* induction by TCDD in zebrafish (*D. rerio*) embryos at 48 and 96 hpf, although a greater overall fold-induction was documented. Similarly, *CYP1A1* levels were elevated in adult mummichogs (*F. heteroclitus*) when exposed to 50 ppb pyrene for 7 days (Roling et al., 2004).

Concurrent with an increase in *CYP1A1* expression with increasing pyrene doses, both pyrene-treated embryos and vehicle controls showed significant increases in *CYP1A1* levels over time of exposure, with the largest fold-induction (~17-fold) occurring in the highest dosage group (150 ppb pyrene) from 24 to 96 hpf (Table 4). In fish, steroid levels increase with development; therefore, increases in *CYP1A1* expression in vehicle-treated embryos with time may be potentially related to the gene's endogenous role in steroid metabolism (Brooks, 1995). Although previous studies have determined that pyrene is a weaker AHR ligand than other environmental contaminants, it was still able to induce *CYP1A1* at low concentrations (20 ppb pyrene) in embryonic *C. variegatus* in the current study, indicating that pyrene binds to and activates the AHR.

3.5. Effect of pyrene exposure on hypoxia-inducible gene expression

In vertebrates, hypoxia *in situ* can occur during anemia or from the external environment (i.e. water) when dissolved

oxygen is <2 mg/L (Brauner and Wang, 1997). Found in vertebrates and invertebrates, the vascular endothelial growth factor gene (*VEGF*) plays a significant role in regulating angiogenesis (Zetter, 1998) during prolonged tissue hypoxia. Unlike the *CYP1A1* gene that is up-regulated when the transcription factor AHR binds to the ARNT protein, *VEGF* is induced when the transcription factor HIF-1 α heterodimerizes with the ARNT protein. Since ARNT is a general dimeric partner for both pathways, the pyrene-activation of the AHR pathway may in turn disrupt the HIF pathway, resulting in decreased *VEGF* expression. Thus, we chose to measure the relative expression of *VEGF* in pyrene-exposed sheepshead minnow embryos and larvae. In all instances, seawater and vehicle treatments showed no significant differences in *VEGF* expression (data not shown); therefore, for all time points, expression of *VEGF* was based on differences between vehicle and pyrene treatments. Q-PCR showed that *VEGF* expression increased significantly in a time-dependent manner for vehicle treatments (Table 5).

Relative to 12 hpf, *VEGF* was induced approximately 5-fold in sheepshead minnow embryos exposed to vehicle for 432 hpf. The hypoxia-inducible gene *VEGF* is thus transcribed under conditions where the external environment is normoxic, suggesting that the oxygen tension in developing tissues is reduced to a level that prevents HIF degradation resulting in *VEGF* transcription. These findings indicate that *VEGF* is involved in development of the vascular system of *C. variegatus* larvae in normoxic waters. Treatment with pyrene did not reduce the endogenous/developmental induction of *VEGF* over time during exposure. Similar to the vehicle control at 96 hpf (3-fold), *VEGF* was induced approximately 3-, 2-, and 3-fold in embryos exposed to 20, 60, and 150 ppb pyrene, respectively, relative to 12 hpf.

While we found no significant differences in *VEGF* regulation among pyrene treatment groups (Table 4), other studies have shown the opposite. Ivnitcki-Steele and Walker (2003) showed a reduction in *VEGF* mRNA and protein expression in chicken embryo hearts after TCDD exposure. Prasch et al. (2004) also found dissimilar results for the hypoxia-inducible gene, heme

Table 5
VEGF normalized fold-change of pyrene-exposed *C. variegatus*

Time	DMSO	20 ppb pyrene	60 ppb pyrene	150 ppb pyrene
12	1.00±0.2	1.19±0.2	1.51±0.2	1.11±0.3
24	1.47±0.2 ^w	1.56±0.2 ^w	1.83±0.2 ^w	1.72±0.1 ^w
48	2.24±0.5 ^{wx}	2.50±0.3 ^{wx}	2.72±0.3 ^{wx}	3.15±0.4 ^{wx}
96	3.13±0.3 ^{wxy}	3.30±1.0 ^{wxy}	3.16±0.2 ^{wxy}	3.38±0.5 ^{wx}
432	5.36±0.7 ^{wxyz}	5.15±1.3 ^{wxyz}	7.08±1.2 ^{wxyz}	m

VEGF normalized fold-change measured using Q-PCR relative to 12 hpf DMSO treatment. Data is presented as mean starting quantity (SQ) [*VEGF*/18S] ($n=4$).

m — 100% mortality before conclusion of exposure at 432 hpf.

No significant differences were found among treatments at any of the five time points, as determined by ANOVA.

Changes within treatments over time:

^w significantly different from same treatment at 12 hpf.

^x significantly different from same treatment at 24 hpf.

^y significantly different from same treatment at 48 hpf.

^z significantly different from same treatment at 96 hpf.

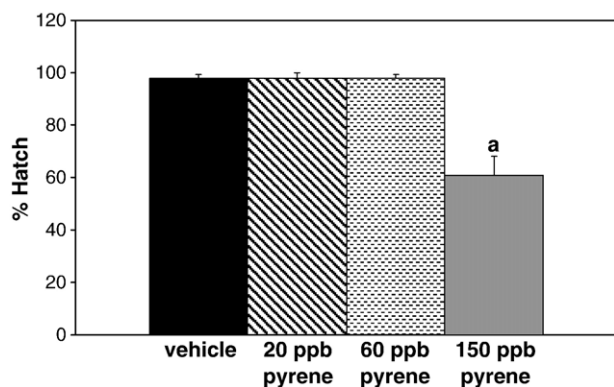


Fig. 1. Percent hatch of pyrene-treated embryos. Treatment groups are: vehicle, 20, 60, and 150 ppb pyrene. Embryos (100 embryos/treatment/time point) were treated with pyrene (20, 60, 150 ppb) or vehicle within 4 hpf for 18 dpf. Data represent the percent hatch for each treatment group and are expressed as mean \pm standard error ($n=4$ tanks/treatment). "a" indicates significant difference from vehicle, 20 ppb pyrene treatment, and 60 ppb pyrene treatment, as determined by Kruskal-Wallis ANOVA on Ranks followed by Tukey post-hoc, where $p \leq 0.05$.

oxygenase. Results demonstrated that heme oxygenase was significantly up-regulated in TCDD-treated zebrafish embryos at 48 hpf under normoxic conditions. In the same study, Prasad et al. (2004) also showed that TCDD did not reduce hypoxia mediated induction of heme oxygenase. Thus, while it appears that expression of hypoxia-inducible genes can be altered by AHR ligands (TCDD), we demonstrated that pyrene does not alter VEGF expression in embryonic sheepshead minnows. Since HIF protein is degraded under normoxic conditions, with HIF mRNA being more or less constant in higher terrestrial vertebrates, it might be argued that increased transcription of VEGF in *C. variegatus* during development is mediated by transcription factors other than HIF/ARNT, which may explain why pyrene does not affect VEGF transcription. However, several recent studies show that HIF protein in fish may occur at much higher oxygen levels than in higher vertebrates. HIF-1 α protein accumulates in rainbow trout and Chinook salmon cells maintained in 5% O₂, an oxygen tension typical of venous blood in normoxic animals, suggesting a role for oxygen dependent gene regulation not only during environmental hypoxia, but also in the normal physiology of these fish (Soitamu et al., 2001). In addition, HIF-1 α , 2 α , and 4 α mRNA in fish are up-regulated in hypoxia, suggesting transcriptional, in addition to post-translational control of HIF in fish (Rahman and Thomas, 2007; Law et al., 2006). Taken together, our results could simply indicate that under our experimental conditions (i.e., exogenous activation of the AHR pathway) there is no competition between AHR and HIF for ARNT heterodimerization, since the numbers of ARNT proteins are likely sufficient for normal developmental HIF-signaling.

3.6. Effect of pyrene exposure on hatch success and survival

Embryonic *C. variegatus*, exposed to seawater, vehicle, 20, 60, or 150 ppb pyrene for 432 hpf were also scored for 1) delayed hatching and hatch success, 2) survival (pre- and post-hatch) up to 432 hpf, and 3) developmental toxicity including

yolk-sac/pericardial edema, skeletal defects such as lordosis, scoliosis, and kyphosis (dorsal body curvature), and retarded growth in the head and trunk region of F0 generation fry. Embryos/larvae were removed with their surrounding water for observations and then returned to their corresponding treatments within approximately 5 min. In all instances, seawater and vehicle treatments showed no significant differences in hatch success, survival, or developmental anomalies (data not shown); therefore, all statistical significance was based on differences between vehicle and pyrene treatments.

In ideal conditions, sheepshead minnows hatch five to six days after fertilization (Kuntz, 1916). For this current study, we observed a typical hatch time of 5 dpf for all treatment groups regardless of pyrene dosage. However, embryos treated with the highest concentration of pyrene (150 ppb) exhibited a 39% decrease in hatch success compared to a 2% loss observed in the 20 and 60 ppb doses (Fig. 1).

This reduction in hatch success indicates that exposure to 150 ppb pyrene, delays and/or halts development in embryonic sheepshead minnows and that the chorionic membrane does not act as a protective barrier against the chemical stressor. Similarly, hatch success of lake herring (*Coregonus artedii*) was reduced by 48% after exposure to TCDD (2,090 $\mu\text{g/g}$ wet weight) for 9 days (Elonen et al., 1998), and a delayed hatch time occurred in steelhead trout (*Salmo gairdneri*) exposed to benzo(a)pyrene (20 $\mu\text{g/L}$) (Kocan and Landolt, 1984).

Survival (pre- and post-hatch) of pyrene-exposed embryos was monitored through 18 dpf (Fig. 2). We observed a dose-dependent increase in mortality over the number of days of exposure. While low levels of pyrene (up to 20 ppb) did not result in significant embryonic mortality through 18 dpf, a significant mortality of remaining pyrene-treated *C. variegatus* was seen in the early days post-hatch. Fry treated with 150 and

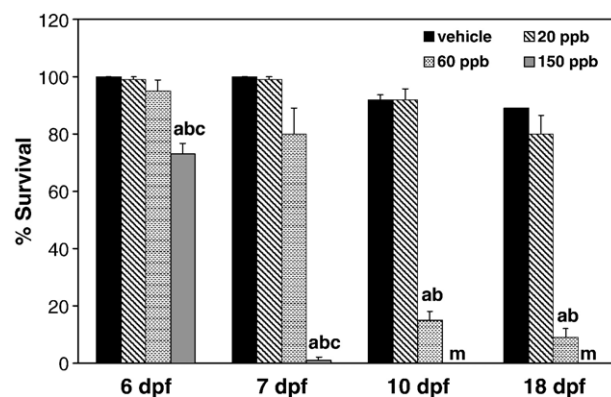


Fig. 2. Percent survival pre- and post-hatch of pyrene-treated *C. variegatus* on 6, 7, 10, and 18 dpf. Embryos (100 embryos/treatment/time point) were treated with pyrene (20, 60, 150 ppb) or vehicle within 4 hpf for 18 dpf. Data represent the percent survival for each treatment at either 6, 7, 10, or 18 dpf and are expressed as mean \pm standard error ($n=4$ tanks/treatment). "a" shows significant difference from same day vehicle control. "b" denotes significant difference from same day 20 ppb pyrene treatment. "c" represents a significant difference from same day 60 ppb treatment. "m" 100% mortality occurred before 10 dpf for 150 ppb pyrene-treated embryos. Statistical significance was determined by ANOVA or Kruskal-Wallis ANOVA on Ranks, followed by Tukey or Student–Newman–Keuls post-hoc tests. In all cases, $p \leq 0.05$.

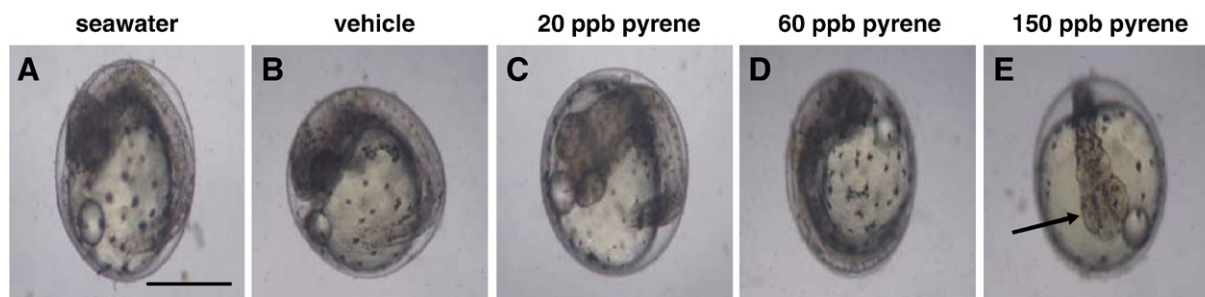


Fig. 3. Effects of pyrene doses on sheephead minnow embryonic development. Shown are 48 hpf embryos after exposure to (A) seawater, (B) vehicle, (C) 20 ppb pyrene, (D) 60 ppb pyrene, and (E) 150 ppb pyrene within 4 hpf. Lack of optical pigmentation (arrow) is indicated in E. Scale bar is 0.5 mm. Embryos shown are representative of four tanks per treatment (100 embryos/treatment).

60 ppb pyrene doses had suffered 100% and 85% mortality by 8 and 10 dpf, respectively.

Similar mortality has been documented in *D. rerio*, where after 96 hours of exposure, zebrafish embryos reared in a nominal concentration of 1000 ppb pyrene (corresponding to ~150 ppb based on solubility of pyrene in water) exhibited 100% mortality by 6 to 7 dpf (Incardona et al., 2004). Thus, it appears *C. variegatus*, along with zebrafish, are more susceptible to pyrene toxicity in the larval stages rather than the embryonic. While in our current study *C. variegatus* treated with 60 ppb pyrene had suffered 91% mortality by 18 dpf, treatment with 20 ppb pyrene resulted in only a 20% loss. Taken together these results indicate that sheephead minnows are capable of tolerating ~20 ppb pyrene in the larval stages, whereas concentrations >60 ppb are lethal.

The mechanism that has been proposed to explain PAH toxicity may also help explain the toxic effect of pyrene observed in our studies. When PAHs diffuse through cellular membranes, enzymes convert non-polar PAHs into polar hydroxy and epoxy derivatives through the induction of microsomal cytochrome P450 monooxygenases and epoxide hydroxylases (WHO, 2000). P450-catalyzed biotransformation of PAHs to toxic metabolites, accompanied by production of reactive oxygen species, can cause developmental, physiological, and cellular toxicity (Ploch et al., 1998). Supporting the link between P450 and developmental toxicity in fish embryos/larvae, exposures of zebrafish, lake trout, and medaka (*O. latipes*) embryos to TCDD result in elevated CYP1A levels, accompanied by various developmental toxicity endpoints (Prasch et al., 2003; Cantrell et al., 1998; Guiney et al., 1997). In our current study, a dose-dependent response for induction of CYP1A1 was closely correlated to the dose-dependent response for larval mortality. At 96 hpf (4 dpf), 150, 60 and 20 ppb pyrene-treated *C. variegatus* had a level of CYP1A1 that was induced ~14-, ~6-, and ~3-fold, respectively, over the vehicle-treated control. Three days later, the 3 exposure groups showed mortalities of 99, 20, and 1%, respectively. This is consistent with reports by Guiney et al. (1997) who found a close correlation in dose-dependency for larval mortality and induction of CYP1A in TCDD-treated lake trout (*Salvelinus namaycush*). Thus, elevated CYP1A1 levels may be linked to increased larval mortality in pyrene-exposed *C. variegatus*; however, the precise mechanism remains undetermined.

3.7. Effects of pyrene on developmental toxicity

608

Embryonic *C. variegatus* were also scored for the presence/absence of developmental abnormalities every 24 h in their

610

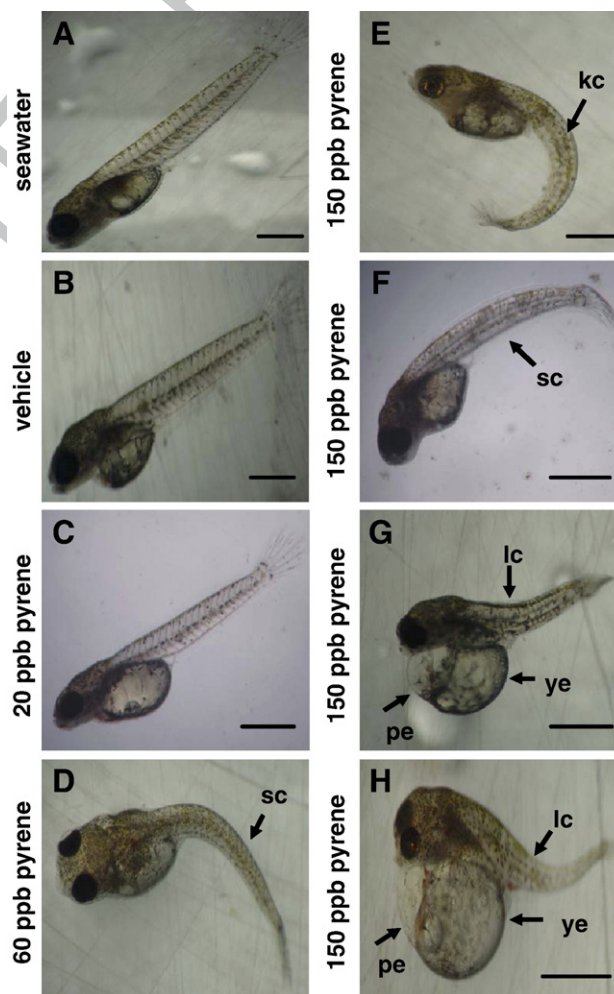


Fig. 4. Effects of pyrene doses on larval development. Shown are 1 dpf larvae after exposure to (A) seawater, (B) vehicle, (C) 20 ppb pyrene, (D) 60 ppb pyrene, and (E–H) 150 ppb pyrene within 4 hpf. Scoliosis curvature (sc) was observed in 60 (D) and 150 ppb (F) pyrene doses. Kyphosis (kc) and lordosis curvatures (lc) are shown in 150 ppb pyrene-exposed larvae (E, G, H). Pericardial (pe) and yolk-sac edema (ye) were observed in 150 ppb pyrene doses (G, H). Scale bars are 0.5 mm. Larvae shown are representative of four replicates per treatment (100 embryos/treatment).

Treatment	Total fry	Average standard length [mm]
Seawater	93	5.93±0.07
Vehicle	88	5.87±0.13
20 ppb pyrene	80	5.09±0.12 ^a
60 ppb pyrene	9	na
150 ppb pyrene	m	m

Data shown are representative of four tanks per treatment as mean±standard error.

na — not applicable; too few fry remaining at conclusion of exposure (432 hpf) to determine accurate measurement.

m — 100% mortality occurred before 432 hpf.

^a Significantly different ($p \leq 0.05$) from both seawater and vehicle treatments as determined by ANOVA followed by Dunn's post-hoc test.

surrounding vehicle/pyrene treatment waters through 432 hpf. Normal embryonic/larval developmental patterns outlined by Kuntz (1916) were used for comparison. Upon hatching, larvae were monitored and scored for the presence/absence of yolk-sac/pericardial edema, dorsal body curvature, and abnormal growth in the head and trunk region. Embryos treated with seawater (Fig. 3A), vehicle (~0.1% DMSO) (Fig. 3B), 20 ppb (Fig. 3C), and 60 ppb (Fig. 3D) pyrene showed grossly normal anatomic developmental patterns through 5 dpf. Though not significant ($p > 0.05$), the earliest observed defect in embryos treated with 150 ppb pyrene was observed at 48 hpf by the lack of pigmentation in the optical region (Fig. 3E).

Upon hatching, larvae treated with vehicle (Fig. 4B) were indistinguishable from larvae reared in seawater (Fig. 4A) alone, demonstrating that there was no effect of DMSO on the development of *C. variegatus* both in the embryonic and larval stages. Larvae in 20 ppb pyrene (Fig. 4C) were almost identical to larvae grown in vehicle-water only. While showing no signs of irregular development, newly hatched 20 ppb pyrene-treated larvae (Fig. 4C) measured ~3 mm in total length as compared to 4 mm seen in vehicle fry on 1 dph. Teraoka et al. (2002) showed a similar but smaller reduction in total body length in TCDD (>0.3 ppb) exposed zebrafish embryos at 72–84 hpf. At 432 hpf, standard length measurements were taken for seawater, vehicle, and 20 ppb pyrene-treated fry. The average standard length of fry treated with 20 ppb pyrene (5.09 mm) was significantly smaller (13–14%) than the seawater and vehicle controls at 432 hpf (Table 6). Thus, even at the lowest concentration (20 ppb), pyrene significantly affects normal larval growth in sheepshead minnows.

While 20 ppb pyrene-exposed larvae showed mostly normal developmental patterns, larvae treated with 60 and 150 ppb pyrene showed significant signs of dose-dependent gross malformations. Approximately 95% of 150 ppb pyrene-treated larvae displayed signs of dorsal curvature of the body and trunk region along with a significant reduction in growth of the head ($p \leq 0.05$). Symptoms ranged from severe curvature of the spine, i.e. kyphosis, lordosis (Fig. 4E, G, H), to having a laterally bent body, i.e. scoliosis (Fig. 4F). Larvae reared in 60 ppb pyrene also showed signs of scoliosis curvature; however, the number of fry displaying symptoms was less

(10%) (Fig. 4D). Though not significant, 150 ppb pyrene-treated fry (5%) also showed pericardial and yolk-sac edema (Fig. 4G, H). The mild edema and explicit dorsal curvature found in the 150 ppb pyrene treatments was comparable with type to a previous study in which *D. rerio* were exposed to ~150 ppb pyrene (not measured, but calculated from the solubility of pyrene in water; Incardona et al., 2004). Thus, it appears that *C. variegatus*, along with zebrafish, show prominent developmental defects in response to pyrene treatment. In conclusion, we showed that increasing doses of pyrene caused an elevation of CYP1A1 levels that preceded or accompanied an increase in severity of developmental abnormalities in larval *C. variegatus*, suggesting a possible role for CYP1A1 in pyrene-mediated embryo toxicity. These results are similar to those reported by Guiney et al. (1997, 2000), who showed increases in vascular permeability and sac-fry mortality following CYP1A induction in early life-stages of TCDD-treated lake trout.

4. Conclusions

Overall, this study was the first to report on the morphological, physiological, and molecular effects on the early life-stages of the sheepshead minnow following early-life stage exposure to pyrene. Significant findings included: developmental anomalies (dorsal curvature/reduced growth) of fry; significant dose-dependent larval mortality; strong induction of PAH-activated gene *CYP1A1*; and pyrene-independent increases in *CYP1A1* and *VEGF* transcription during development from the embryonic to larval stages. Since *VEGF* transcription is not affected by pyrene, we tentatively conclude that levels of intracellular ARNT are sufficient to support both AHR-activated transcription of *CYP1A1* and endogenously-controlled transcription of *VEGF*. The studies reported here have laid the groundwork for examination of the combined effects of hypoxia and pyrene (two common environmental stressors) on the embryonic sheepshead minnow (Hendon, 2006).

5. Uncited references

Henry et al., 1997

Jeziarska et al., 2000

Wisk and Cooper, 1990

Acknowledgments

This work was supported by grants (NA04NOS4260203 and NA05NOS4261163) from the National Oceanic and Atmospheric Administration Coastal Ocean Program. Embryo exposure protocols received prior approval from the University of Southern Mississippi Institutional Animal Care and Use Committee (#121 R02). The authors would like to thank Rachel Ryan for all her technical expertise and assistance in the molecular part of this project, Dr. Jonathan Roling for his help and advice with Q-PCR, and Thea Hoexum-Brouwer for assistance with HPLC.

References

- Achenbach, J.E., Topliff, C.L., Vassilev, V.B., Donis, R.O., Eskridge, K.M., Kelling, C.L., 2004. Detection and quantitation of bovine respiratory syncytial virus using real-time quantitative RT-PCR and quantitative competitive RT-PCR assays. *J. Virol. Methods* 121, 1–6.
- Andreasen, E.A., Hahn, M.E., Heideman, W., Peterson, R.E., Tanguay, R.L., 2002a. The zebrafish (*Danio rerio*) aryl hydrocarbon receptor type 1 is a novel vertebrate receptor. *Mol. Pharmacol.* 62, 234–249.
- Andreasen, E.A., Spitsbergen, J.M., Tanguay, R.L., Stegeman, J.J., Heideman, W., Peterson, R.E., 2002b. Tissue-specific expression of AHR2, ARNT2, and CYP1A in zebrafish embryos and larvae: effects of developmental stage and 2,3,7,8-tetrachlorodibenzo-*p*-dioxin exposure. *Toxicol. Sci.* 68, 403–419.
- Barron, M.G., Heintz, R., Rice, S.D., 2004. Relative potency of PAHs and heterocycles as aryl hydrocarbon receptor agonists in fish. *Mar. Environ. Res.* 58, 95–100.
- Brauner, C.J., Wang, T., 1997. The optimal oxygen equilibrium curve: a comparison between environmental hypoxia and anemia. *Am. Zool.* 37, 101–108.
- Brooks, G.T., 1995. Cytochrome P450: Structure, Mechanism, and Biochemistry, 2nd ed. Plenum Press, New York.
- Cantrell, S.M., Joy-Schlezing, J., Stegeman, J.J., Tillitt, D.E., Hannink, M., 1998. Correlation of 2,3,7,8-tetrachlorodibenzo-*p*-dioxin-induced apoptotic cell death in the embryonic vasculature with embryo toxicity. *Toxicol. Appl. Pharmacol.* 148, 24–34.
- Denison, M.S., Pandini, A., Nagy, S.R., Baldwin, E.P., Bonati, L., 2002. Ligand binding and activation of the Ah receptor. *Chem.-Biol. Interact.* 141, 3–24.
- Elonen, G.E., Spehar, R.L., Holcombe, G.W., Johnson, R.D., Fernandez, J.D., Erickson, R.J., Tietge, J.E., Cook, P.M., 1998. Comparative toxicity of 2,3,7,8-tetrachlorodibenzo-*p*-dioxin to seven freshwater fish species during early life stage development. *Environ. Toxicol. Chem.* 17, 472–483.
- Forsythe, J.A., Jiang, B.H., Iyer, N.V., Agani, F., Leung, S.W., Koos, R.D., Semenza, G.L., 1996. Activation of vascular endothelial growth factor gene transcription by hypoxia inducible factor 1. *Mol. Cell. Biol.* 16, 4605–4613.
- Gong, B., Liang, D., Chew, T.G., Ge, R., 2004. Characterization of the zebrafish vascular endothelial growth factor A gene: comparison with vegf-A genes in mammals and Fugu. *Biochim. Biophys. Acta* 1676, 33–40.
- Guiney, P.D., Smolowitz, R.M., Peterson, R.E., Stegeman, J.J., 1997. Correlation of 2,3,7,8-tetrachlorodibenzo-*p*-dioxin induction of cytochrome P4501A in vascular endothelium with toxicity in early life stages of lake trout. *Toxicol. Appl. Pharmacol.* 143, 256–273.
- Guiney, P.D., Walker, M.K., Spitsbergen, J.M., Peterson, R.E., 2000. Hemodynamic dysfunction and cytochrome P4501A mRNA expression induced by 2,3,7,8-tetrachlorodibenzo-*p*-dioxin during embryonic stages of lake trout development. *Toxicol. Appl. Pharmacol.* 168, 1–14.
- Hahn, M.E., 2002. Aryl hydrocarbon receptor: diversity and evolution. *Chem.-Biol. Interact.* 141, 131–160.
- Hendon, L.A., 2006. Cross-talk between pyrene and hypoxia signaling pathways in embryonic *Cyprinodon variegatus*. MS thesis. University of Southern Mississippi, Ocean Springs, MS.
- Henry, T.R., Spitsbergen, J.M., Hornung, M.W., Abnet, C.C., Peterson, R.E., 1997. Early life stage toxicity of 2,3,7,8-tetrachlorodibenzo-*p*-dioxin in zebrafish (*Danio rerio*). *Toxicol. Appl. Pharmacol.* 142, 56–68.
- Holmes, D.I.R., Zachary, Ian., 2005. The vascular endothelial growth factor (VEGF) family: angiogenic factors in health and disease. *Genome Biol.* 6, 209.
- Incardona, J.P., Collier, T.K., Scholz, N.L., 2004. Defects in cardiac function precede morphological abnormalities in fish embryos exposed to polycyclic aromatic hydrocarbons. *Toxicol. Appl. Pharmacol.* 196, 191–205.
- Ivnitski-Steele, I.D., Walker, M.K., 2003. Vascular endothelial growth factor rescues 2,3,7,8-tetrachlorodibenzo-*p*-dioxin inhibition of coronary vasculogenesis. *Birth Defects Res. Part A. Clin. Mol. Teratol.* 67, 496–503.
- Jezierska, B., Lugowska, K., Witeska, M., Samowski, P., 2000. Malformations of newly hatched common carp larvae. *Electron. J. Pol. Agric. Univ., Fish.* 3 (2).
- Kocan, R.M., Landolt, M.L., 1984. Alterations in patterns of excretion and other metabolic functions in developing fish embryos exposed to benzo(a)pyrene. *Helgol. Mar. Res.* 37, 493–504.
- Kuntz, A., 1916. Notes on the embryology and larval development of five species of teleostean fishes. *Bull. U.S. Bur. Fish.* 34, 409–429.
- Law, S.H.W., Wu, R.S.S., Ng, P.K.S., Yu, R.M.K., Kong, R.Y.C., 2006. Cloning and expression analysis of two distinct HIF- α isoforms -gcHIF-1 α and gcHIF-4 α — from the hypoxia tolerant grass carp, *Ctenopharyngodon idellus*. *BMC Mol. Biol.* 7, 15.
- Lee, P.J., Jiang, B.H., Chin, B.Y., Iyer, N.V., Alam, J., Semenza, G.L., Choi, A.M., 1997. Hypoxia-inducible factor-1 mediates transcriptional activation of the heme oxygenase-1 gene in response to hypoxia. *J. Biol. Chem.* 272, 5375–5381.
- Manning, C.S., Schesny, A.L., Hawkins, W.E., Barnes, D.H., Barnes, C.S., Walker, W.W., 1999. Exposure methodologies and systems for long-term chemical carcinogenicity studies with small fish species. *Toxicol. Methods* 9, 201–217.
- Morita, T., Perrella, M.A., Lee, M.E., Kourembanas, S., 1995. Smooth muscle cell-derived carbon monoxide is a regulator of vascular cGMP. *Proc. Natl. Acad. Sci. U. S. A.* 92, 1475–1479.
- National Research Council, 2003. Oil in the Sea III: Inputs, Fates, and Effects. National Academies Press, Washington, D.C.
- Nebert, D.W., Roe, A.L., Dieter, M.Z., Solis, W.A., Yang, Y., Dalton, T.P., 2000. Role of the aromatic hydrocarbon receptor and the Ah gene battery in the oxidative stress response, cell cycle control, and apoptosis. *Biochem. Pharmacol.* 59, 65–85.
- Ploch, S.A., King, L.C., Kohan, M.J., Di Giulio, R.T., 1998. Comparative in vitro and in vivo benzo[a]pyrene-DNA adduct formation and its relationship to CYP1A activity in two species of ictalurid catfish. *Toxicol. Appl. Pharmacol.* 149, 90–98.
- Prasch, A.L., Teraoka, H., Carney, S.A., Dong, W., Hiraga, T., Stegeman, J.J., Heiderman, W., Peterson, R.E., 2003. Aryl hydrocarbon receptor 2 mediates 2,3,7,8-Tetrachlorodibenzo-*p*-dioxin developmental toxicity in zebrafish. *Toxicol. Sci.* 76, 138–150.
- Prasch, A.L., Andreasen, E.A., Peterson, R.E., Heideman, W., 2004. Interactions between 2,3,7,8-tetrachlorodibenzo-*p*-dioxin (TCDD) and hypoxia signaling pathways in zebrafish: hypoxia decreases responses to TCDD in zebrafish embryos. *Toxicol. Sci.* 78, 68–77.
- Rahman, M.S., Thomas, P., 2007. Molecular cloning, characterization and expression of two hypoxia-inducible factor alpha subunits, HIF-1 α and FIF-2 α , in a hypoxia-tolerant marine teleost, Atlantic croaker (*Micropogonias undulatus*). *Gene*. doi:10.1016/j.gene.2007.03.009.
- Roling, J.A., Bain, L.J., Baldwin, W.S., 2004. Differential gene expression in mummichogs (*Fundulus heteroclitus*) following treatment with pyrene: comparison to a creosote contaminated site. *Mar. Environ. Res.* 57, 377–395.
- Safe, S., Wormke, M., Samudio, I., 2000. Mechanisms of inhibitory aryl hydrocarbon receptor–estrogen receptor crosstalk in human breast cancer cells. *J. Mammary Gland Biol. Neoplasia* 5, 295–296.
- Semenza, G.L., 1999. Regulation of mammalian O₂ homeostasis by hypoxia-inducible factor 1. *Annu. Rev. Cell Dev. Biol.* 15, 551–578.
- Semenza, G.L., 2000. HIF-1 and human disease: one highly involved factor. *Genes Dev.* 14, 1983–1991.
- Semenza, G.L., Wang, G.L., 1992. A nuclear factor induced by hypoxia via de novo protein synthesis binds to the human erythropoietin gene enhancer at a site required for transcriptional activation. *Mol. Cell. Biol.* 12, 5447–5454.
- Soitamu, A.J., Rabergh, C.M.I., Gassmann, M., Sistonen, L., Nikinmaa, M., 2001. Characterization of a hypoxia-inducible factor (HIF-1 α) from rainbow trout. *J. Biol. Chem.* 276, 19699–19705.
- Tanguay, R.L., Abnet, C.C., Heideman, W., Peterson, R.E., 1999. Cloning and characterization of the zebrafish (*Danio rerio*) aryl hydrocarbon receptor. *Biochim. Biophys. Acta* 1444, 35–48.
- Teraoka, H., Dong, W., Ogawa, S., Tsukiyama, S., Okuhara, Y., Niyama, M., Ueno, N., Peterson, R.E., Hiraga, T., 2002. 2,3,7,8-Tetrachlorodibenzo-*p*-dioxin toxicity in the zebrafish embryo: altered regional blood flow and impaired lower jaw development. *Toxicol. Sci.* 65, 192–199.
- United States Environmental Protection Agency, 2000. Naval Station Mayport: Project XL-Final Project Agreement. <http://www.epa.gov/projectxl/mayport/fpa.pdf>.
- United States Environmental Protection Agency, 2002. Short-term methods for estimating the chronic toxicity of effluents and receiving waters to marine and estuarine organisms, 3rd ed. EPA-821-R-02-014.

- 837 United States Environmental Protection Agency, 2006. Current national
838 recommended water quality criteria. Health and Ecological Criteria
839 Division, Office of Science and Technology. EPA. 822-R-02-047.
- 840 Wisk, J.D., Cooper, K.R., 1990. The stage specific toxicity of 2,3,7,8-
841 tetrachlorodibenzo-p-dioxin in embryos of the Japanese medaka (*Oryzias*
842 *latipes*). Environ. Toxicol. Chem. 9, 1159–1169.
- World Health Organization, 2000. Polycyclic aromatic hydrocarbons (PAH), In: 843
Theakston, F. (Ed.), Air Quality Guidelines, 2nd ed. World Health 844
Organization, Copenhagen, Denmark, pp. 1–24. 845
- Zetter, B.R., 1998. Angiogenesis and tumor metastasis. Annu. Rev. Med. 49, 846
407–424. 847

UNCORRECTED PROOF